55 $[(CH_3)_2NH_2]_2CoCl_4$ family

55A Pure compounds

No. 55A-1 $[(CH_3)_2NH_2]_2CoCl_4$, Dimethylammonium tetrachlorocobaltate (II)

(M = 292.93)

1a Possibility of ferroelectricity in $[(CH_3)_2NH_2]_2CoCl_4$ was mentioned by Vasil'ev et al. in 1987. 87Vas

b

phase	IV [a])	III [b])	II	I [c])
state	P	(F)	P	
crystal system	monoclinic	monoclinic		
space group	$P12_1/n1 - C_{2h}^5$ [d])	$P12_1/n1 - C_{2h}^5$ [e])		
Θ [K]	≈238 [a])	≈260 [b])	≈419 [c])	

[a]) 86Bob
[b]) 87Vas
[c]) 96Kap
[d]) 92Wil
[e]) 89Ole

Anomalies in dielectric constants, heat capacity and birefringence have been reported at about 187, 313, 353 and 380 K: see subsections 5a, 6a and 9a.

$\rho_X = 1.50 \cdot 10^3$ kg m^{-3} at T = 295(1) K. 92Wil

Deep dark blue. 91Tor

Hygroscopic. 91Tor

2a Crystal growth: evaporation method from aqueous solution containing stoichiometric molar ratio of $(CH_3)_2NH_2Cl$ and $CoCl_2$. 89Ole

b Orthogonal coordinate system is defined as follows: X and Y axes are parallel to the acute and obtuse bisectrices of the optic axes, respectively; Z axis is parallel to the b axis. 92Vlo

3a Unit cell parameters:
a = 8.541(1) Å, b = 11.440(2) Å, c = 13.311(2) Å, β = 90.02(1)° at T = 295(1) K; 92Wil
a = 7.803(2) Å, b = 11.285(3) Å, c = 14.523(4) Å, β = 96.11(2)° at T = 220(5) K;
see also 89Ole

b Z = 4 in phase II [a]) and phase IV [b]). [a]) 89Ole [b]) 92Wil

Positional and temperature parameters: Table 55A-1-001, Table 55A-1-002.
Interatomic distances and angles: Table 55A-1-003.
Crystal structure: Fig. 55A-1-001, Fig. 55A-1-002.

4 Thermal expansion: see 86Bob, 96Kap

5a Dielectric constant: Fig. 55A-1-003, Fig. 55A-1-004, Fig. 55A-1-005, Fig. 55A-1-006.
Dielectric dispersion: Fig. 55A-1-007, Fig. 55A-1-008, Fig. 55A-1-009, Fig. 55A-1-010; see also the insert of Fig. 55A-1-005.

c Coercive field: $1.3 \cdot 10^5$ V m^{-1} at T = 260 K. 87Vas

6a Heat capacity: Fig. 55A-1-011; see also 86Bob
Total transition heat and transition entropy for the anomaly of heat capacity in Fig. 55A-1-011: $\Delta Q_m = 1.59 \cdot 10^3$ J mol^{-1}, $\Delta S_m = 6.61$ J mol^{-1} K^{-1}. 87Vas

9a Birefringence: Fig. 55A-1-012.
Optical absorption spectrum: Fig. 55A-1-013.
Infrared reflection spectra: see 92Vlo

10a	Raman scattering: see	91Tor
11	Electrical conductivity: see	95Kap
16	Usually, crystals crack at the phase transition from phase III to IV. Dielectric properties and conductivity are seriously affected by extrinsic water.	87Vas 96Kap

Table 55A-1-001. $[(CH_3)_2NH_2]_2CoCl_4$. Fractional coordinates and equivalent isotropic temperature parameters [Å^2] in phase II at 295(1) K [92Wil]. $U_{eq} = \Sigma U_{ii}/3$, where U_{ii} is defined by Eq. (d) in Introduction.

Atom	*x*	*y*	*z*	U_{eq}
Co(1)	0.16965(3)	0.29931(2)	0.41877(2)	0.0401(1)
Cl(1)	0.18100(7)	0.49671(5)	0.40991(5)	0.0564(2)
Cl(2)	0.19215(8)	0.23570(5)	0.58033(4)	0.0556(2)
Cl(3)	–0.07356(7)	0.23748(5)	0.36886(5)	0.0549(2)
Cl(4)	0.36014(8)	0.22076(6)	0.32265(5)	0.0658(2)
N(1)	–0.2073(3)	0.1903(2)	0.5967(2)	0.0599(8)
C(1)	–0.3729(4)	0.2199(4)	0.5814(4)	0.086(2)
C(2)	–0.1741(5)	0.0648(3)	0.6069(3)	0.086(1)
H(11)	–0.148(4)	0.224(3)	0.549(2)	0.075(9)
H(12)	–0.165(5)	0.227(3)	0.646(3)	0.104(14)
N(2)	–0.2108(2)	0.5023(2)	0.3351(2)	0.0550(7)
C(3)	–0.1531(4)	0.5107(3)	0.2314(2)	0.063(1)
C(4)	–0.3794(4)	0.4795(4)	0.3425(3)	0.082(1)
H(21)	–0.152(3)	0.440(3)	0.367(2)	0.080(9)
H(22)	–0.181(5)	0.562(4)	0.366(3)	0.126(15)

Table 55A-1-002. $[(CH_3)_2NH_2]_2CoCl_4$. Fractional coordinates and equivalent isotropic temperature parameters [Å^2] in phase IV at 220(5) K [92Wil]. $U_{eq} = \Sigma U_{ii}/3$, where U_{ii} is defined by Eq. (d) in Introduction.

Atom	*x*	*y*	*z*	U_{eq}
Co(1)	0.20846(3)	0.29455(2)	0.45369(1)	0.0268(1)
Cl(1)	0.21360(5)	0.49525(4)	0.44448(3)	0.0368(1)
Cl(2)	0.17795(5)	0.23773(4)	0.60276(3)	0.0352(1)
Cl(3)	–0.03172(5)	0.022536(4)	0.36683(3)	0.0379(1)
Cl(4)	0.45081(6)	0.21356(4)	0.40832(3)	0.0409(1)
N(1)	–0.2358(2)	0.1928(2)	0.5681(1)	0.0393(5)
C(1)	–0.2986(4)	0.2275(2)	0.6565(2)	0.0541(8)
C(2)	–0.2227(4)	0.0638(2)	0.5546(2)	0.0584(9)
H(11)	–0.305(4)	0.220(2)	0.519(2)	0.076(9)
H(12)	–0.145(4)	0.225(2)	0.570(2)	0.062(8)
N(2)	–0.1947(2)	0.4849(2)	0.3270(1)	0.0348(5)
C(3)	–0.1139(3)	0.5197(2)	0.2438(1)	0.0418(6)
C(4)	–0.3847(3)	0.4801(2)	0.3120(2)	0.0469(7)
H(21)	–0.154(3)	0.414(2)	0.342(2)	0.062(7)
H(22)	–0.171(3)	0.523(2)	0.371(2)	0.058(7)

Table 55A-1-003. $[(CH_3)_2NH_2]_2CoCl_4$. Interatomic distances [Å] and angles [°] in phase II at 295(1) K and phase IV at 220(5) K [92Wil].

	295 K	220 K
Co(1)–Cl(1)	2.264(1)	2.269(1)
Co(1)–Cl(2)	2.278(1)	2.295(1)
Co(1)–Cl(3)	2.293(1)	2.283(1)
Co(1)–Cl(4)	2.257(1)	2.261(1)
N(1)–C(1)	1.468(4)	1.475(3)
N(1)–C(2)	1.471(4)	1.474(3)
N(2)–C(3)	1.469(4)	1.474(3)
N(2)–C(4)	1.468(4)	1.476(3)
Cl(1)–Co(1)–Cl(2)	111.4(1)	109.8(1)
Cl(1)–Co(1)–Cl(3)	109.4(1)	109.1(1)
Cl(1)–Co(1)–Cl(4)	109.7(1)	111.5(1)
Cl(2)–Co(1)–Cl(3)	104.5(1)	105.3(1)
Cl(2)–Co(1)–Cl(4)	110.3(1)	109.6(1)
Cl(3)–Co(1)–Cl(4)	111.5(1)	111.3(1)
C(1)–N(1)–C(2)	115.0(3)	114.3(2)
C(3)–N(2)–C(4)	113.9(2)	113.6(2)

Hydrogen-bond contacts			
295 K		220 K	
H(11)...Cl(3)	2.48(3)	H(11)...Cl(4^{iii})	2.36(3)
H(12)...Cl(4^{i})	2.44(4)	H(12)...Cl(2)	2.52(3)
H(21)...Cl(3)	2.41(4)	H(21)...Cl(3)	2.35(3)
H(22)...Cl(1^{ii})	2.89(4)	H(22)...Cl(1^{ii})	2.72(4)
H(22)...Cl(2^{ii})	2.42(4)	H(22)...Cl(2^{ii})	2.74(4)

Symmetry code: (i) $x - 1/2, 1/2 - y, 1/2 + z$;
(ii) $-x, 1 - y, 1 - z$;
(iii) $x - 1, y, z$.

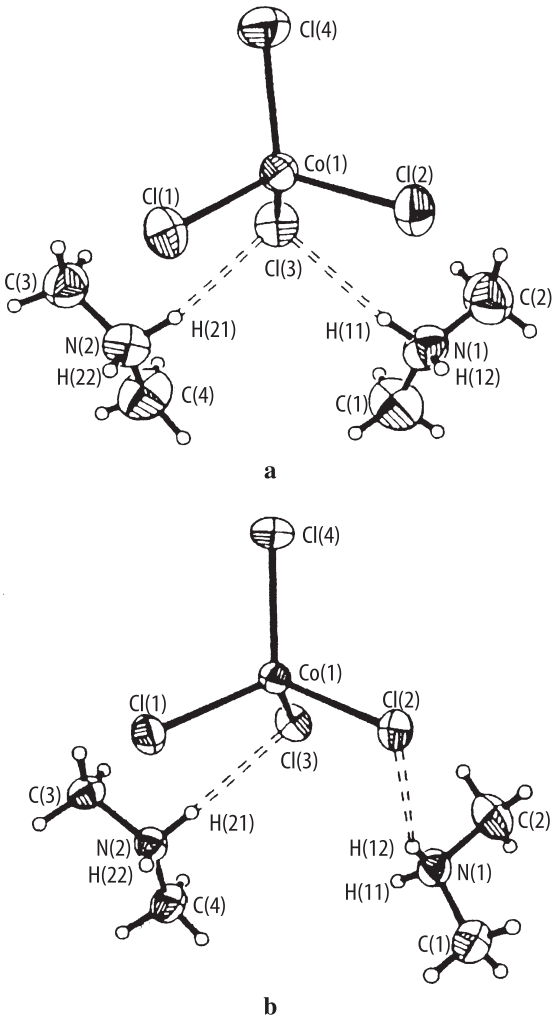

Fig. 55A-1-001. $[(CH_3)_2NH_2]_2CoCl_4$. Molecular structure; (**a**) phase II at 295(1) K, (**b**) phase IV at 220(5) K [92Wil]. Double dashed lines represent hydrogen bonds.

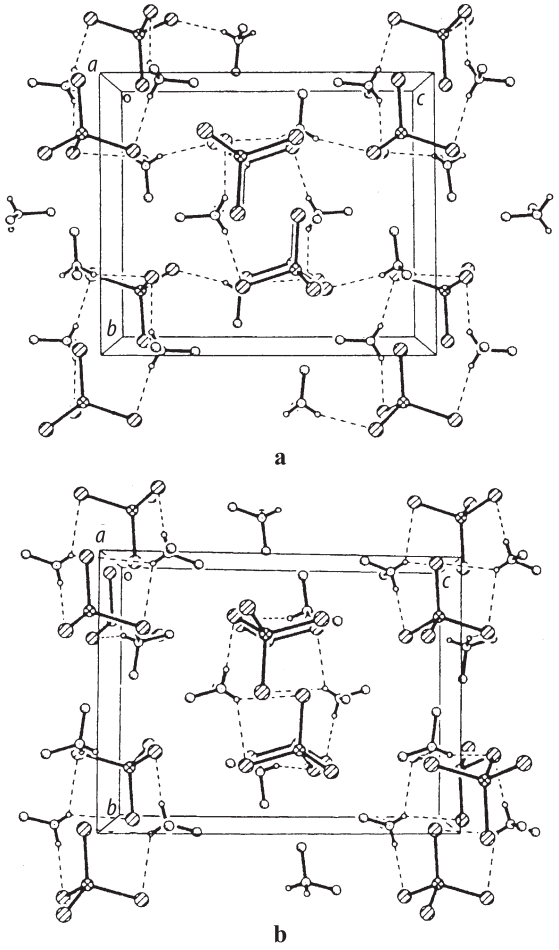

Fig. 55A-1-002. $[(CH_3)_2NH_2]_2CoCl_4$. Perspective view of crystal structure along the *a* axis; (**a**) phase I at 295(1) K, (**b**) phase III at 220(5) K [92Wil]. Dashed lines represent hydrogen bonds.

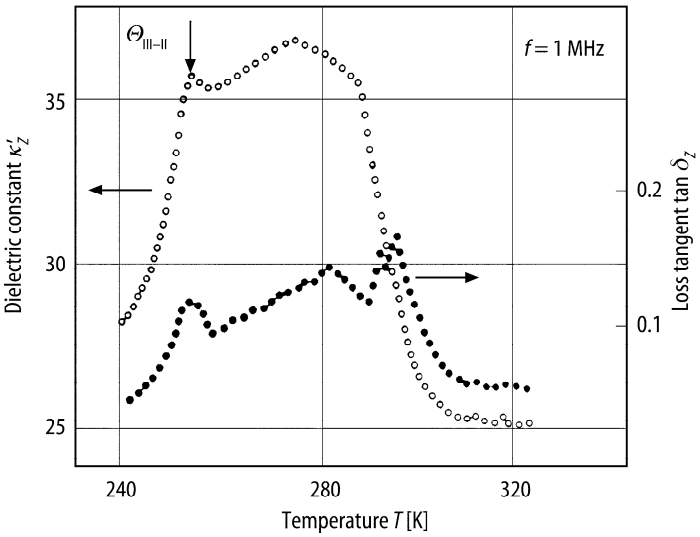

Fig. 55A-1-003. $[(CH_3)_2NH_2]_2CoCl_4$. κ'_Z, tan δ_Z vs. T [95Kap]. tan δ_Z: loss tangent along the Z axis. $f = 1$ MHz.

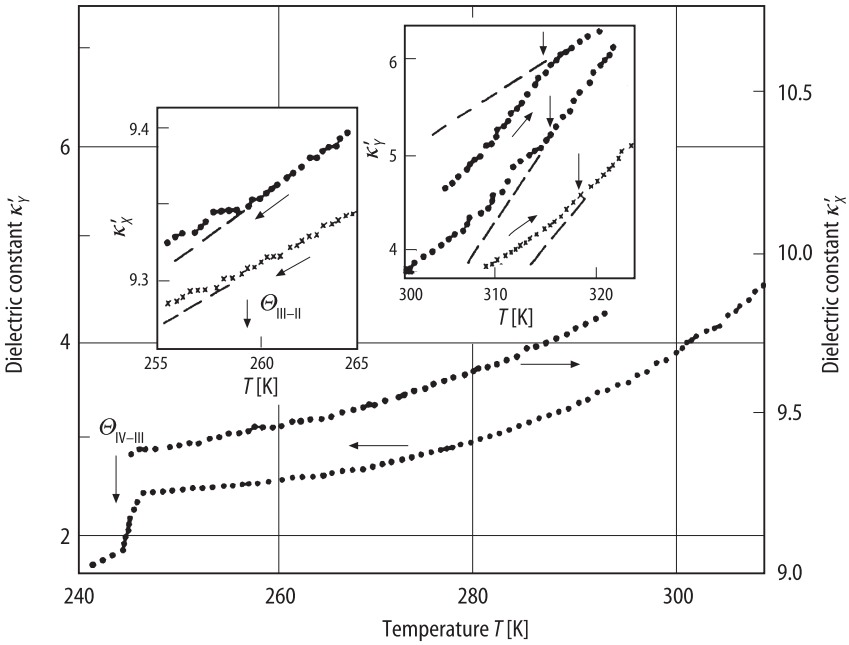

Fig. 55A-1-004. $[(CH_3)_2NH_2]_2CoCl_4$. κ'_X, κ'_Y vs. T [95Kap]. f = 10 kHz (full circle) and 40 kHz (cross). Vertical arrows indicate dielectric anomalies.

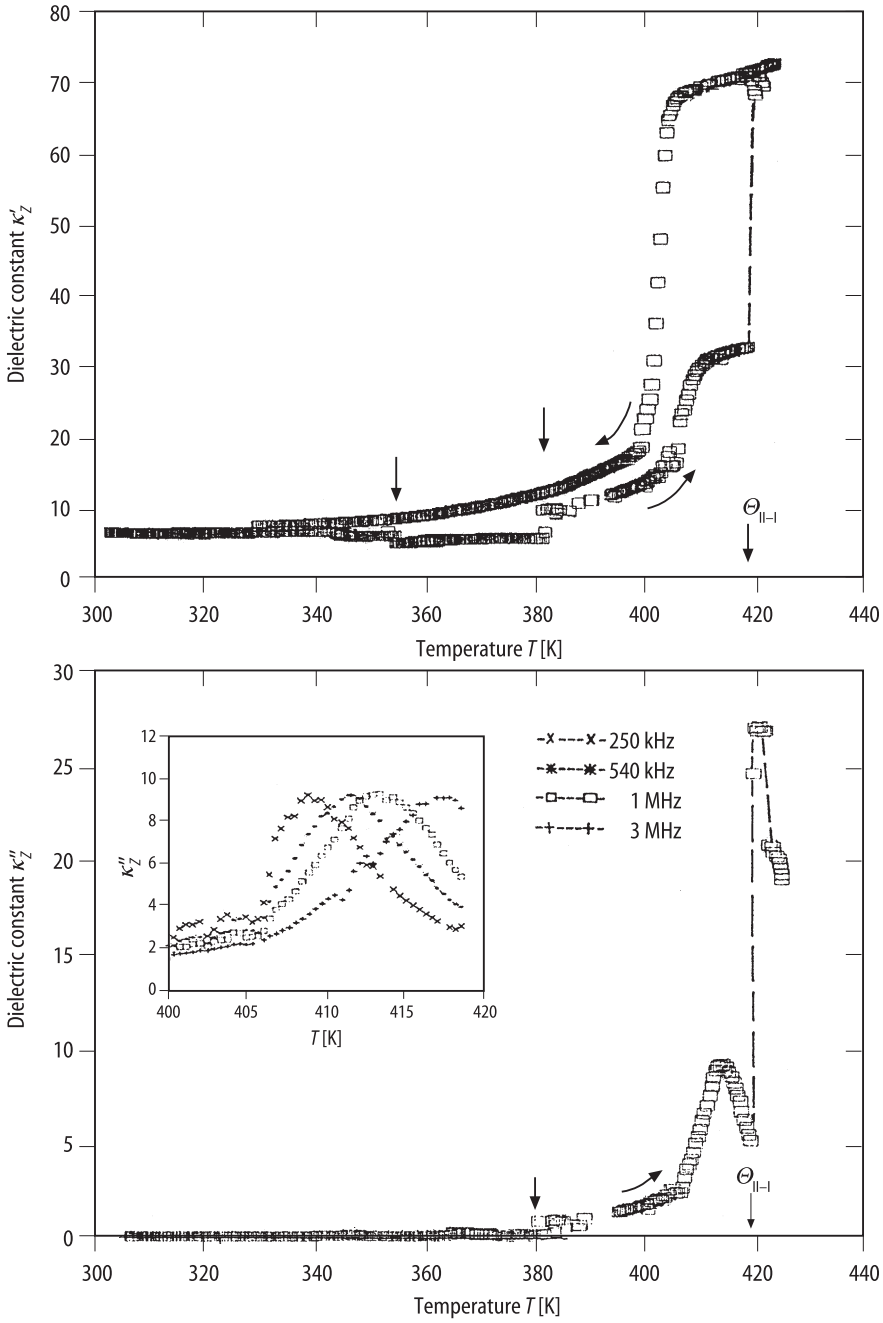

Fig. 55A-1-005. $[(CH_3)_2NH_2]_2CoCl_4$. κ'_Z, κ''_Z vs. T measured in vacuum [96Kap]. f = 1 MHz. Vertical arrows indicate dielectric anomalies. The insert shows dielectric dispersion with parameter f.

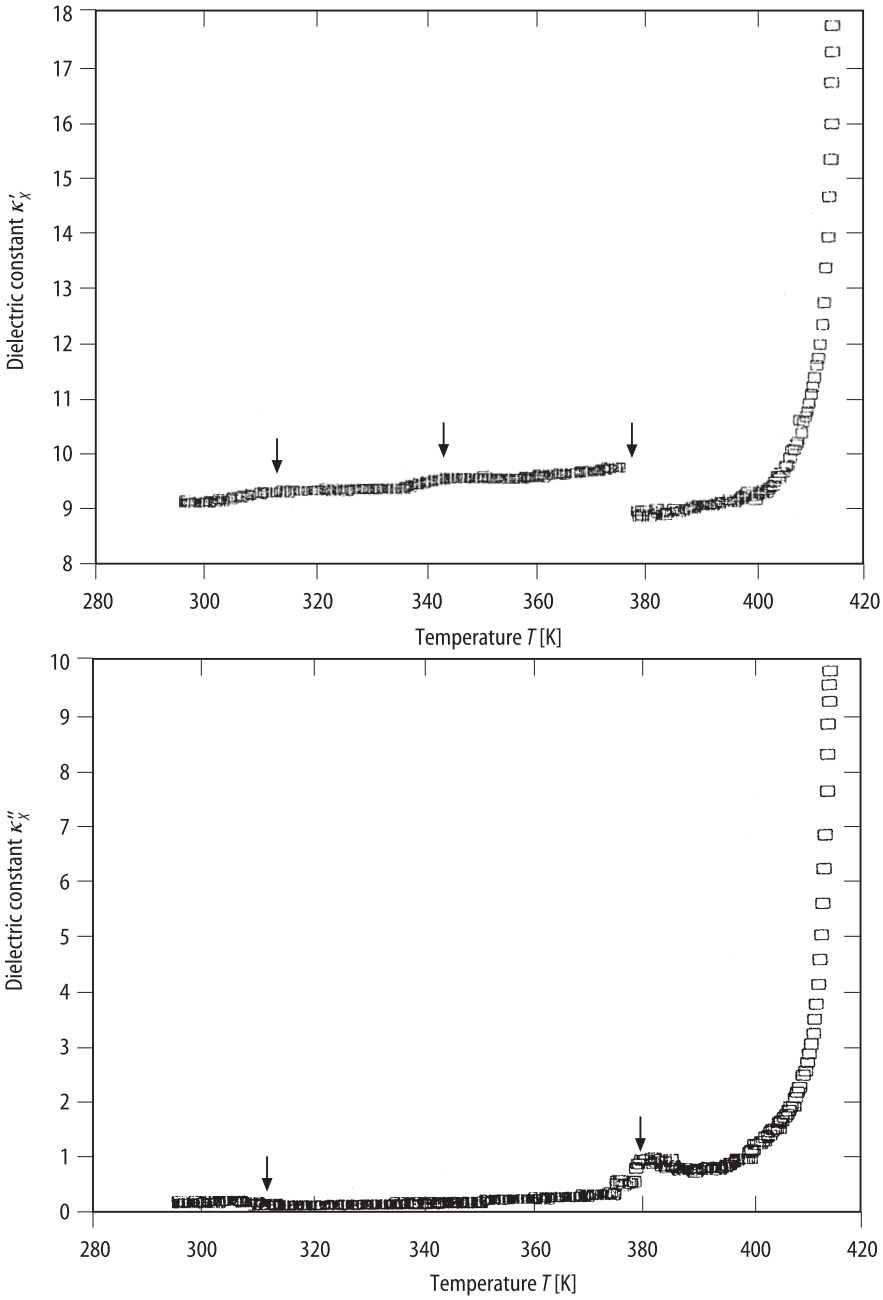

Fig. 55A-1-006. $[(CH_3)_2NH_2]_2CoCl_4$. κ'_X, κ''_X vs. T measured in vacuum [96Kap]. f = 100 kHz. Vertical arrows indicate dielectric anomalies.

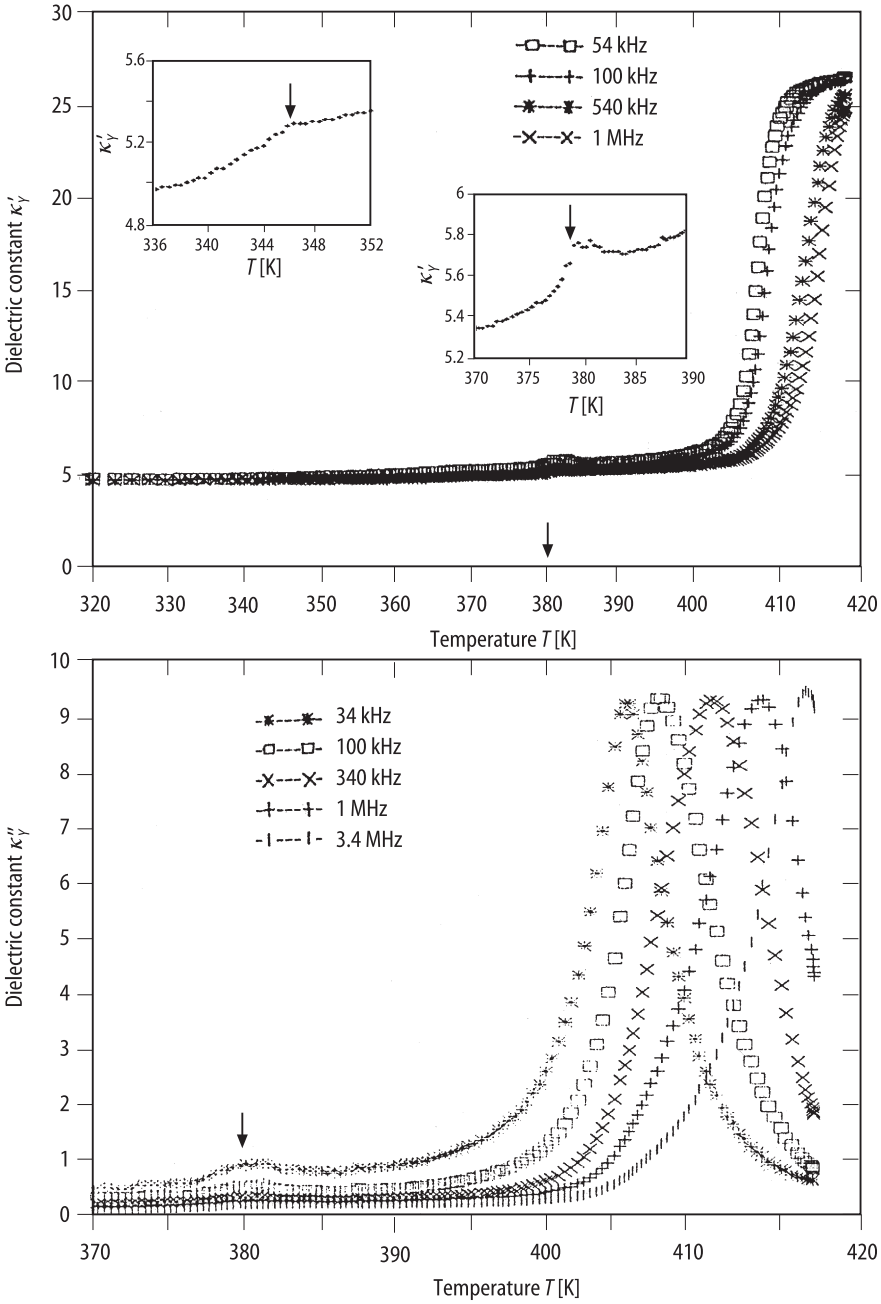

Fig. 55A-1-007. $[(CH_3)_2NH_2]_2CoCl_4$. κ'_Y, κ''_Y vs. T measured in vacuum [96Kap]. Parameter: *f*. Vertical arrows indicate dielectric anomalies.

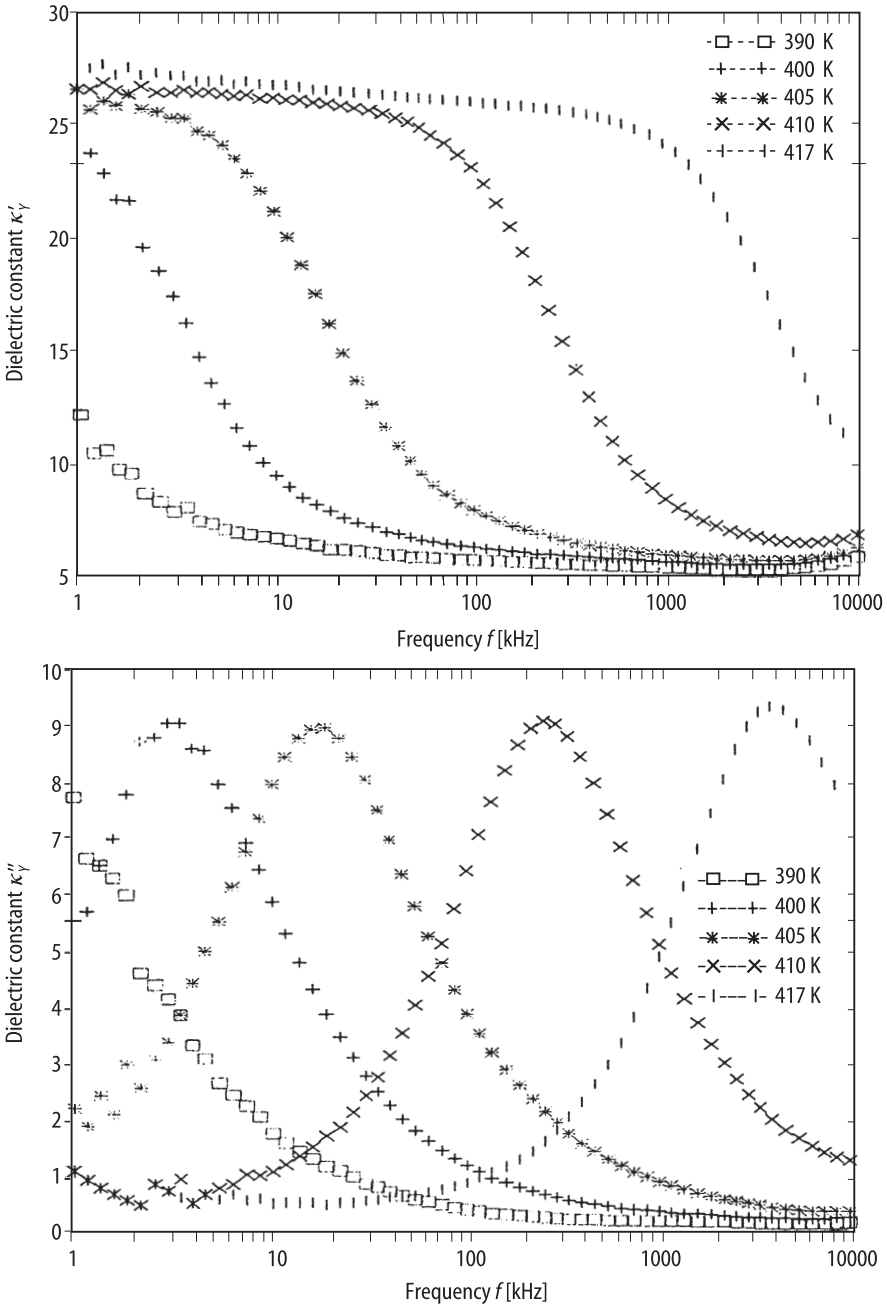

Fig. 55A-1-008. $[(CH_3)_2NH_2]_2CoCl_4$. κ'_Y, κ''_Y vs. f measured in vacuum [96Kap]. Parameter: T.

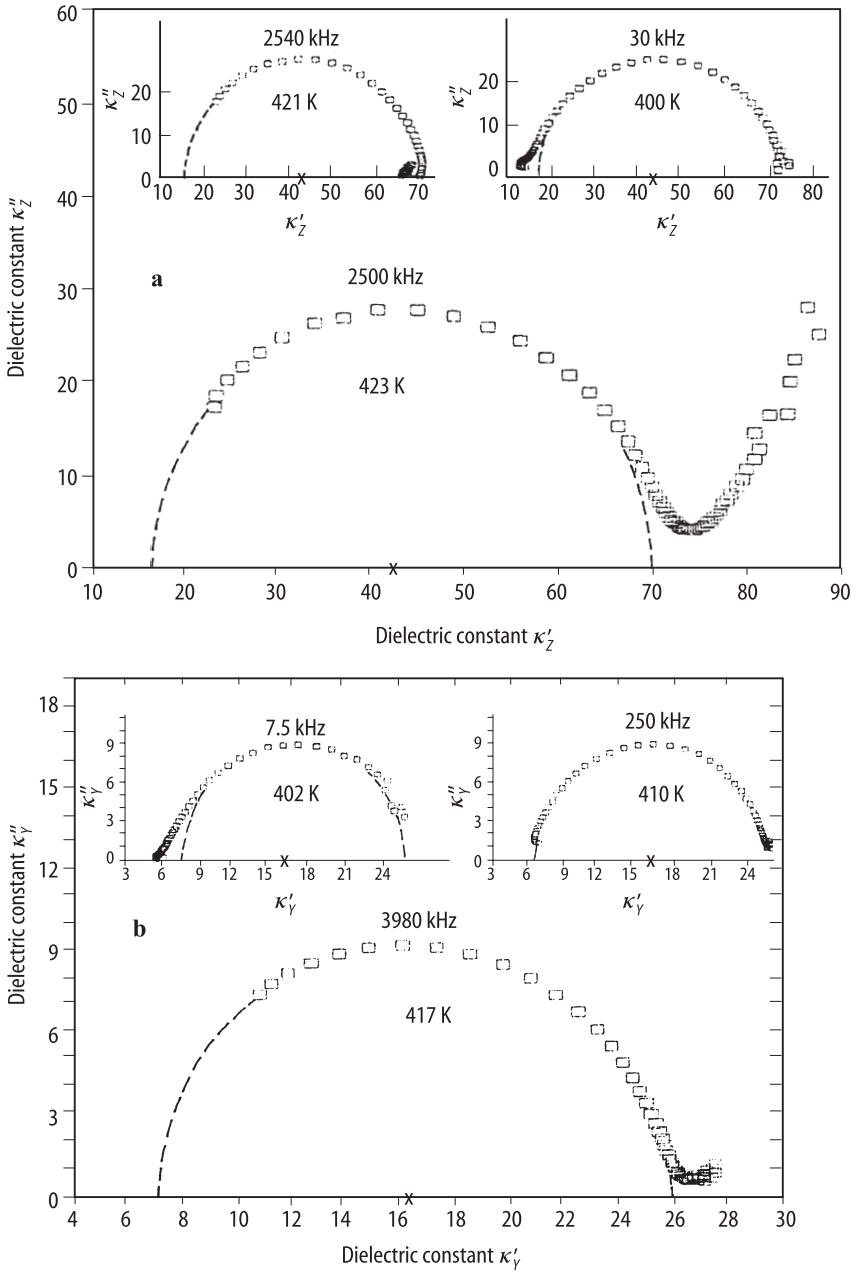

Fig. 55A-1-009. $[(CH_3)_2NH_2]_2CoCl_4$. Cole-Cole plots of the complex dielectric constants measured in vacuum [96Kap]. (**a**) along the *Z* axis on cooling, (**b**) along the *Y* axis on heating. Parameter: *T*. Relaxation frequencies are also noted.

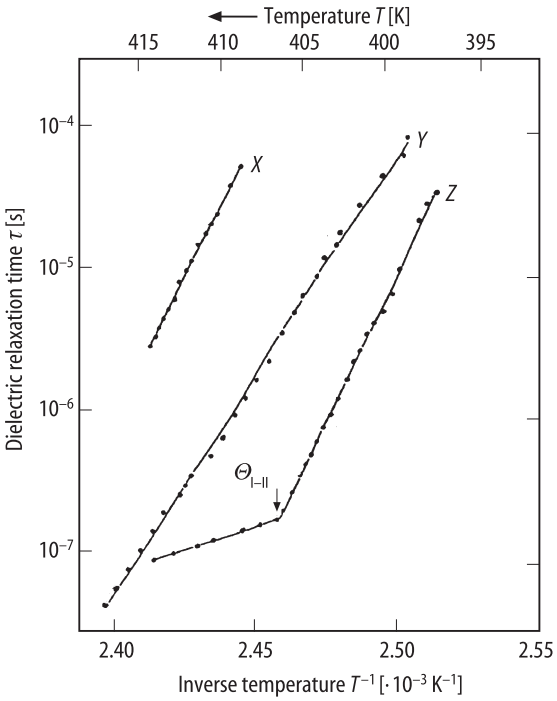

Fig. 55A-1-010. $[(CH_3)_2NH_2]_2CoCl_4$. τ vs. $1/T$ [96Kap]. τ: dielectric relaxation time for *X*-, *Y*- and *Z*-cuts of the crystal. Measurements were done on heating for *X*- and *Y*-cuts, and on cooling for *Z*-cut. Activation energies are 0.66 eV for *X*-cut, 0.57 eV for *Y*-cut, 0.77 eV (below $\Theta_{I–I}$) and 0.11 eV (above $\Theta_{I–I}$) for *Z*-cut, respectively.

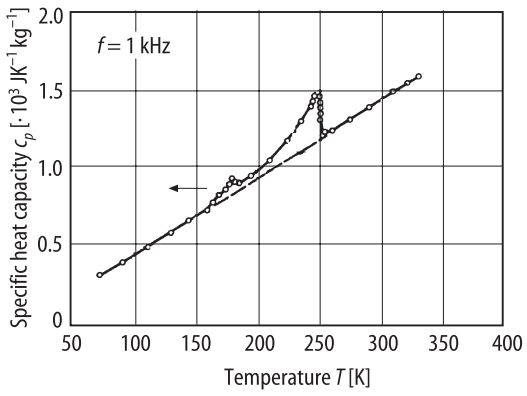

Fig. 55A-1-011. $[(CH_3)_2NH_2]_2CoCl_4$. c_p vs. T [87Vas]. c_p: specific heat capacity at constant pressure.

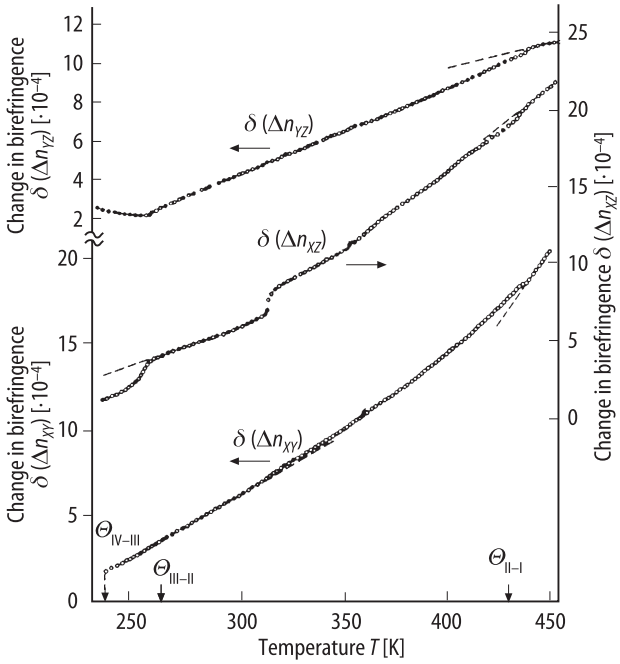

Fig. 55A-1-012. $[(CH_3)_2NH_2]_2CoCl_4$. $\delta(\Delta n_{XY})$, $\delta(\Delta n_{YZ})$, $\delta(\Delta n_{XZ})$ vs. T [92Vlo]. $\delta(\Delta n_{XY})$, $\delta(\Delta n_{YZ})$, $\delta(\Delta n_{XZ})$: change in birefringence in XY, YZ and XZ plane, respectively. $\lambda = 4358$ Å.

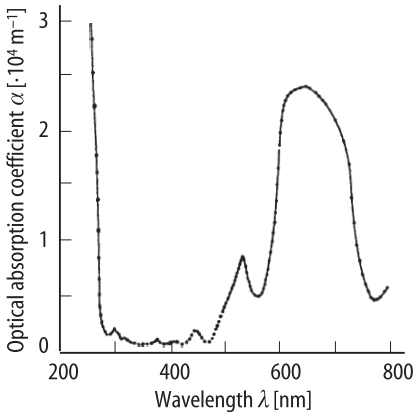

Fig. 55A-1-013. $[(CH_3)_2NH_2]_2CoCl_4$. α vs. λ [92Vlo]. α: optical absorption coefficient for polarized light propagating along the Z axis with $\boldsymbol{E} \parallel \boldsymbol{X}$.

References

86Bob Bobrova, Z.A., Varikash, V.M.: Dokl. Akad. Nauk BSSR **30** (1986) 510.

87Vas Vasil'ev, V.E., Rudyak, V.M., Bobrova, Z.A., Varikash, V.M.: Fiz. Tverd. Tela **29** (1987) 1539; Sov. Phys. Solid State (English Transl.) **29** (1987) 882.

89Ole Oleshchuk, A.Yu., Kiosse, G.A., Bobrova, Z.A., Shuvalov, L.A., Malinovskii, T.I.: Kristallografiya **34** (1989) 1146; Sov. Phys. Crystallogr. (English Transl.) **34** (1989) 690.

91Tor Torgashev, V.I., Yuzyuk, Yu.I., Rabkin, L.M., Durnev, Yu.I., Bobrova, Z.A.: Phys. Status Solidi (b) **168** (1991) 317.

92Vlo Vlokh, O.G., Kapustyanyk, V.B., Mykhalyna, I.A., Polovinko, I.I., Sveleba, S.A., Bobrova, Z.A., Varikash, V.M.: Kristallografiya **37** (1992) 766; Sov. Phys. Crystallogr. (English Transl.) **37** (1992) 403.

92Wil Williams, I.D., Brown, P.W., Taylor, N.J.: Acta Crystallogr. Sect. C **48** (1992) 263.

95Kap Kapustianik, V.B., Sveleba, S.A., Tchukvinskyi, R., Korchak, Yu., Mokryi, V., Polovinko, I.I., Trybula, Z.: Phys. Status Solidi (a) **151** (1995) 481.

96Kap Kapustianik, V.B., Kabelka, H., Warhanek, H., Fuith, A.: Phys. Status Solidi (a) **155** (1996) 95.

No. 55A-2 $[(CH_3)_2NH_2]_2CuCl_4$, Dimethylammonium tetrachlorocuprate (II)

(M = 297.54)

1a Ferroelectric activity in $[(CH_3)_2NH_2]_2CuCl_4$ was discovered by Bobrova et al. in 1987. 87Bob

b

phase	III	II	I
state		F	P
crystal system			orthorhombic
space group			(Pnam– D_{2h}^{16}) [a])
Θ [K]	253.05	279.65	

87Bob

[a]) 88Bob1

Another modification, monoclinic at RT with orange color, has been reported. It undergoes phase transition at 111.5 K: see Fig. 55A-2-005. 94Dzh

Transparent and yellow. 87Bob

2a Crystal growth: evaporation method from aqueous solution containing stoichiometric molar ratio of $(CH_3)_2NH_2Cl$ and $CuCl_2$. 87Bob

b Crystal form: Fig. 55A-2-001.

4 Thermal expansion: Fig. 55A-2-002; see also 86Bob

5a Dielectric constant: Fig. 55A-2-001.

Curie-Weiss constant and temperature: $C = 9 \cdot 10^3$ K, $\Theta_p = 250$ K in phase I. 87Bob

Effect of biasing field on the Curie temperature: $d\Theta_{II-I}/dE_{bias} = 2.32 \cdot 10^{-6}$ K mV^{-1}. 87Bob

Effect of deuteration: Fig. 55A-2-003.

c $P_s = 2.0 \cdot 10^{-2}$ C m^{-2}, $E_c = 6.6 \cdot 10^5$ V m^{-1} at Θ_{II-I}. 87Bob

6a Differential scanning calorimetry: see 86Bob, 88Bob2

Transition heat and transition entropy: Table 55A-2-001.

9a Birefringence: Fig. 55A-2-004.

Birefringence of the second modification: Fig. 55A-2-005.

Absorption in visible region: Fig. 55A-2-006.

b Electrooptic effect: Fig. 55A-2-007.

10a Raman scattering: see 94Dzh

Table 55A-2-001. $[(CH_3)_2NH_2]_2CuCl_4$, $[(CH_3)_2NH_{2-x}D_x]_2CuCl_4$. Transition temperature, transition heat and transition entropy measured by differential scanning calorimetry [88Bob2]. x was not determined.

Crystal	Θ [K]	ΔQ_m [J mol^{-1}]	ΔS_m [J K^{-1} mol^{-1}]
$[(CH_3)_2NH_2]_2CuCl_4$	279	535	1.92
	253	547	2.18
$[(CH_3)_2NH_{2-x}D_x]_2CuCl_4$	275	413	1.50
	255	480	1.88

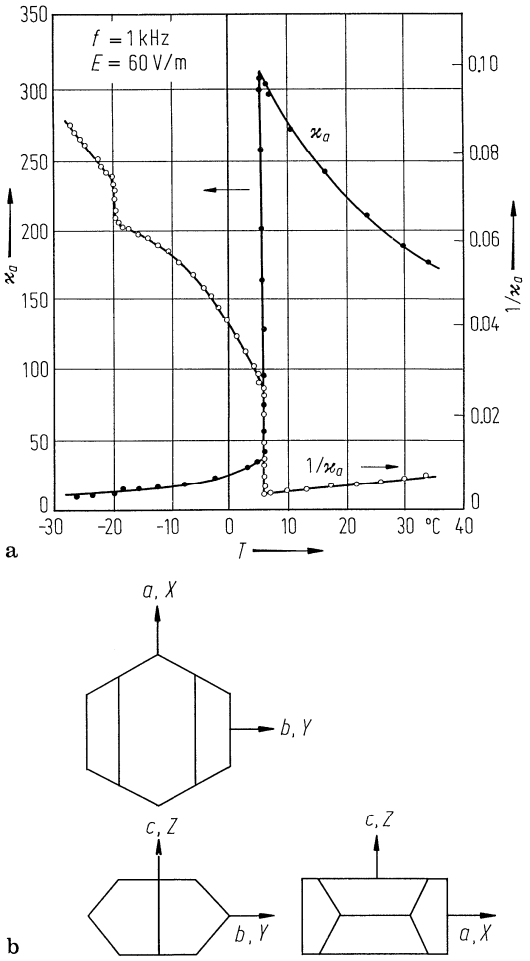

Fig. 55A-2-001. $[(CH_3)_2NH_2]_2CuCl_4$. κ_a, $1/\kappa_a$ vs. T (**a**) [87Bob]. The crystallographic axes a, b, c are assigned as shown in (**b**).

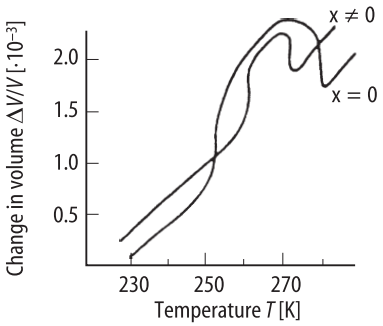

Fig. 55A-2-002. $[(CH_3)_2NH_{2-x}D_x]_2CuCl_4$. $\Delta V/V$ vs. T [88Bob2]. ΔV: change in volume. x was not determined.

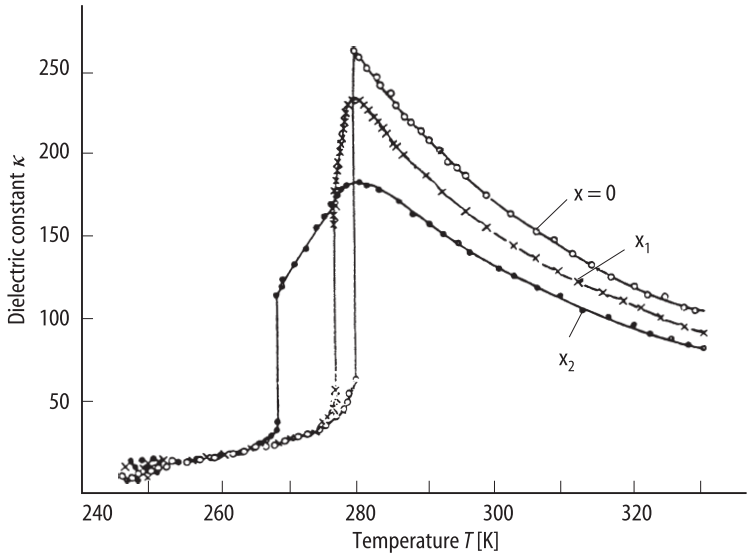

Fig. 55A-2-003. $[(CH_3)_2NH_{2-x}D_x]_2CuCl_4$. κ vs. T [88Bob2]. Parameter: x. $x_1 < x_2$.

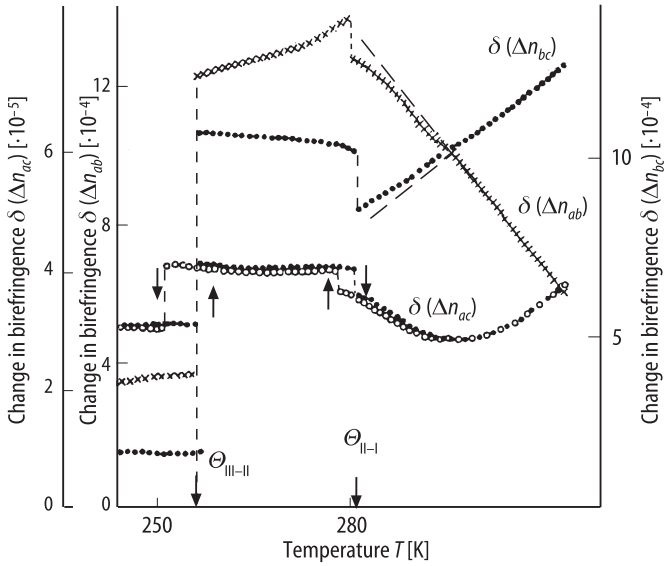

Fig. 55A-2-004. $[(CH_3)_2NH_2]_2CuCl_4$. $\delta(\Delta n_{ab})$, $\delta(\Delta n_{bc})$, $\delta(\Delta n_{ac})$ vs. T [89Vlo]. $\delta(\Delta n_{ab})$, $\delta(\Delta n_{bc})$, $\delta(\Delta n_{ac})$: change in birefringence in *ab*, *bc* and *ac* plane, respectively.

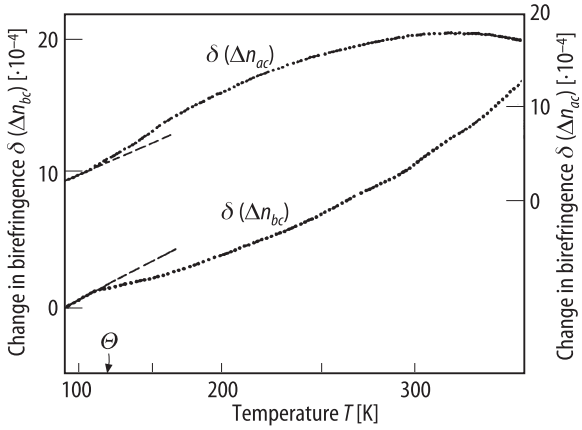

Fig. 55A-2-005. $[(CH_3)_2NH_2]_2CuCl_4$. $\delta(\Delta n_{bc})$, $\delta(\Delta n_{ac})$ vs. T in the second modification [92Kap]. $\delta(\Delta n_{bc})$, $\delta(\Delta n_{ac})$: change in birefringence in *bc* and *ac* plane, respectively.

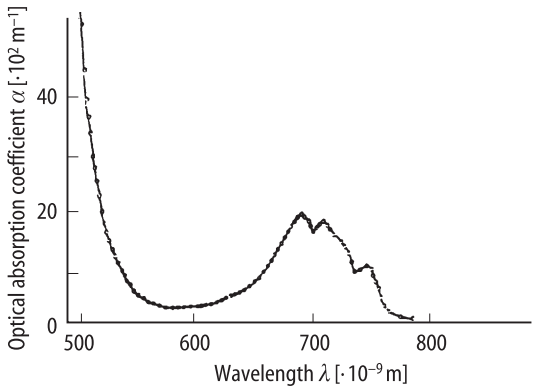

Fig. 55A-2-006. $[(CH_3)_2NH_2]_2CuCl_4$. α vs. λ [92Vlo]. α: optical absorption coefficient for polarization $\boldsymbol{E} \parallel \boldsymbol{b}$.

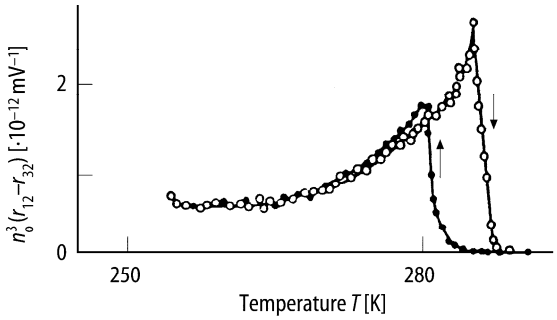

Fig. 55A-2-007. $[(CH_3)_2NH_2]_2CuCl_4$. $n_o^3(r_{12} - r_{32})$ vs. T [89Vlo]. $r_{\lambda i}$: electrooptic constant.

References

86Bob Bobrova, Z.A., Varikash, V.M.: Dokl. Akad. Nauk BSSR **30** (1986) 510.

87Bob Bobrova, Z.A., Varikash, V.M., Baranov, A.I., Shuvalov, L.A.: Kristallografiya **32** (1987) 255; Sov. Phys. Crystallogr. (English Transl.) **32** (1987) 148.

88Bob1 Bobrova, Z.A., Varikash, V.M., Akimova, N.E.: Abstracts of Papers presented at Fourth All-Union School-Seminar on Ferroelastics (1988) 169; a work cited in [89Vlo].

88Bob2 Bobrova, Z.A., Varikash, V.M.: Fiz. Tverd. Tela **30** (1988) 2629; Sov. Phys. Solid State (English Transl.) **30** (1988) 1514.

89Vlo Vlokh, O.G., Varikash, V.M., Bobrova, Z.A., Kapustyanyk, V.B., Polovinko, I.I., Sveleba, S.A.: Fiz. Tverd. Tela **31** (1989) 264; Sov. Phys. Solid State (English Transl.) **31** (1989) 1250.

92Kap Kapustianik, V.B., Polovinko, I.I., Sveleba, S.A., Vlokh, O.G., Bobrova, Z.A., Varikash, V.M.: Phys. Status Solidi (a) **133** (1992) 45.

92Vlo Vlokh, O.G., Kapustyanyk, V.B., Polovinko, I.I., Sveleba, S.A., Bobrova, Z.A., Varikash, V.M.: Zh. Prikl. Spektrosk. **56** (1992) 86; J. Appl. Spectrosc. (English Transl.) **56** (1992) 64.

94Dzh Dzhala, V., Kapustianik, V., Kityk, I., Polovinko, I., Sveleba, S.: Ferroelectrics **152** (1994) 273.

No. 55A-3 $[(CH_3)_2NH_2]_2ZnCl_4$, Dimethylammonium tetrachlorozincate (II)

(M = 299.39)

1b	Crystal system is monoclinic with space group $P112_1/n - C_{2h}^5$ at RT.	89Ole
	Phase sequence has not been established.	
	Transparent, colorless.	91Tor
	$\rho_X = 1.51 \cdot 10^3$ kg m^{-3} at T = 296 K.	89Ole
2a	Crystal growth: evaporation method from aqueous solution containing stoichiometric molar ratio of $(CH_3)_2NH_2Cl$ and $ZnCl_2$.	89Ole
b	Orthogonal coordinate system is defined as follows: X and Y axes are parallel to the obtuse and acute bisectrices of the optic axes, respectively.	90Vlo
3a	Unit cell parameters: a = 13.297(9) Å, b = 8.620(7) Å, c = 11.494(3) Å, γ = 89.9° at T = 296 K.	89Ole
b	Z = 4 at 296 K.	89Ole
	Positional and temperature parameters: Table 55A-3-001.	
	Interatomic distances and angles: Table 55A-3-002.	
	Crystal structure: Fig. 55A-3-001.	
4	Thermal expansion: see	86Bob
6a	Heat capacity: Fig. 55A-3-002, Fig. 55A-3-003; see also	86Bob
9a	Birefringence: Fig. 55A-3-004.	
	Absorption spectrum in visible and ultraviolet region: Fig. 55A-3-005.	
c	Piezooptic effect: Fig. 55A-3-006.	
10a	Raman scattering: see	91Tor
13a	^{35}Cl NQR: Fig. 55A-3-007, Fig. 55A-3-008.	

Table 55A-3-001. $[(CH_3)_2NH_2]_2ZnCl_4$. Fractional coordinates [$\cdot 10^{-4}$] and mean square thermal displacements [$\cdot 10^{-2}$ Å^2] at 296 K [89Ole].

Atom	x	y	z	$\overline{u^2}$
Zn	813(0)	3285(1)	2012(1)	3.65
Cl(1)	1315(1)	5722(2)	2629(1)	5.14
Cl(2)	–806(1)	3068(2)	2629(1)	5.12
Cl(3)	1773(1)	1396(2)	2806(2)	6.18
Cl(4)	908(1)	3188(2)	45(1)	5.25
N(1)	837(4)	2906(6)	12(5)	5.07
C(1)	7305(5)	3470(9)	94(7)	6.10
C(2)	8421(7)	1183(9)	–224(9)	8.06
N(2)	4021(4)	2059(7)	1924(5)	5.73
C(3)	3880(7)	1747(13)	620(7)	9.15
C(4)	830(7)	1249(10)	–2811(8)	8.19

Table 55A-3-002. $[(CH_3)_2NH_2]_2ZnCl_4$. Interatomic distances and angles at 296 K [89Ole].

Interatomic distances [Å]		Angles [°]	
Zn–Cl(1)	2.319(2)	Cl(2)–Zn–Cl(1)	104.7(1)
Zn–Cl(2)	2.275(2)	Cl(3)–Zn–Cl(1)	111.5(1)
Zn–Cl(3)	2.258(2)	Cl(3)–Zn–Cl(2)	110.4(1)
Zn–Cl(4)	2.267(1)	Cl(4)–Zn–Cl(1)	108.8(1)
		Cl(4)–Zn–Cl(2)	110.2(1)
		Cl(4)–Zn–Cl(3)	110.2(1)
N(1)–C(1)	1.477(9)	C(2)–N(1)–C(1)	112.7(6)
N(1)–C(2)	1.489(10)	C(3)–N(2)–C(4)	110.5(5)
N(2)–C(3)	1.494(11)		
N(2)–C(4)	1.473(10)		

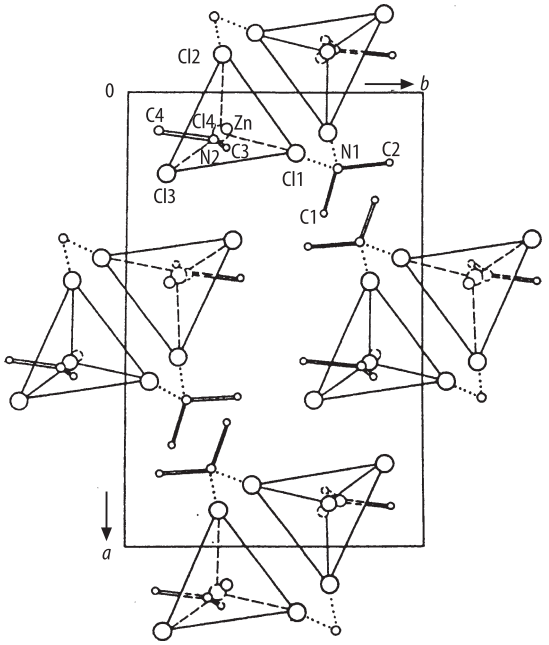

Fig. 55A-3-001. $[(CH_3)_2NH_2]_2ZnCl_4$. Crystal structure at 296 K [89Ole]. Projection along the *c* axis.

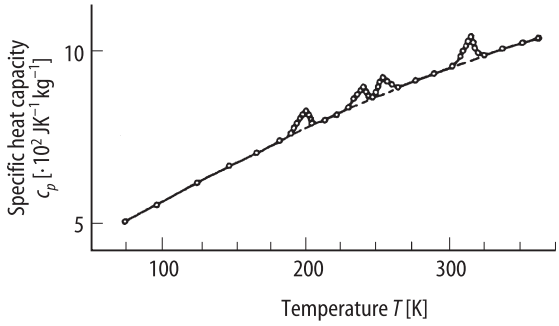

Fig. 55A-3-002. $[(CH_3)_2NH_2]_2ZnCl_4$. c_p vs. T [87Vas]. c_p: specific heat capacity at constant pressure.

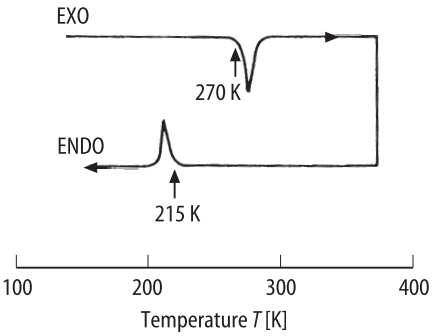

Fig. 55A-3-003. $[(CH_3)_2NH_2]_2ZnCl_4$. DTA curves [90Yam]. EXO: exothermic. ENDO: endothermic.

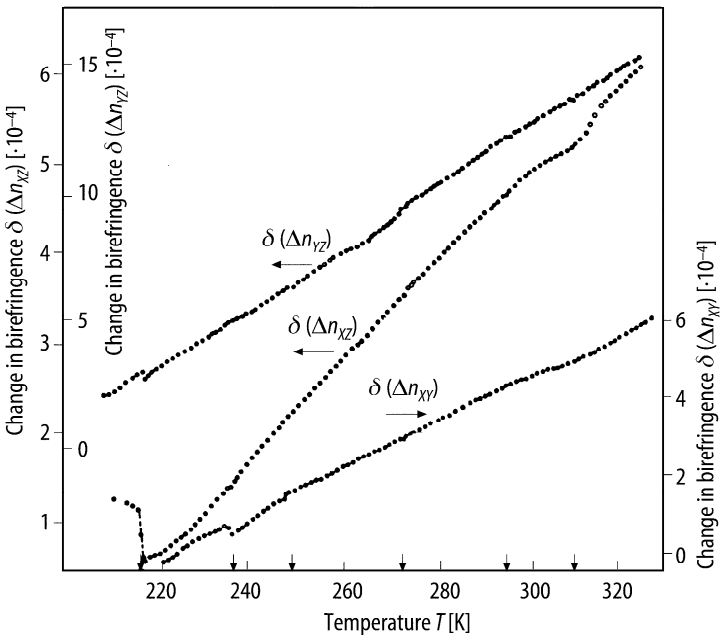

Fig. 55A-3-004. $[(CH_3)_2NH_2]_2ZnCl_4$. $\delta(\Delta n_{XY})$, $\delta(\Delta n_{YZ})$, $\delta(\Delta n_{XZ})$ vs. T [90Vlo]. $\delta(\Delta n_{XY})$, $\delta(\Delta n_{YZ})$, $\delta(\Delta n_{XZ})$: change in birefringence in XY, YZ and XZ plane, respectively. λ = 6328 Å.

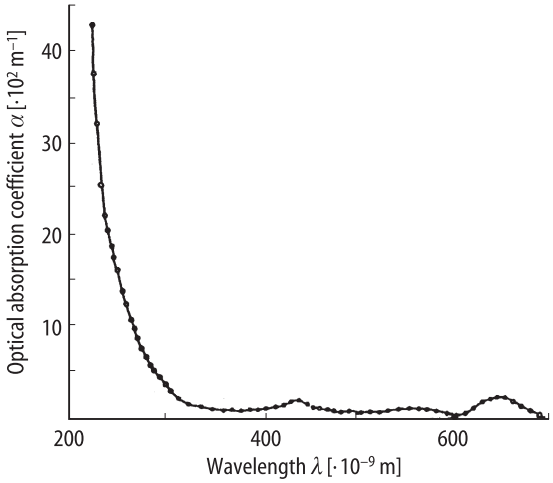

Fig. 55A-3-005. $[(CH_3)_2NH_2]_2ZnCl_4$. α vs. λ [90Vlo]. α: optical absorption coefficient.

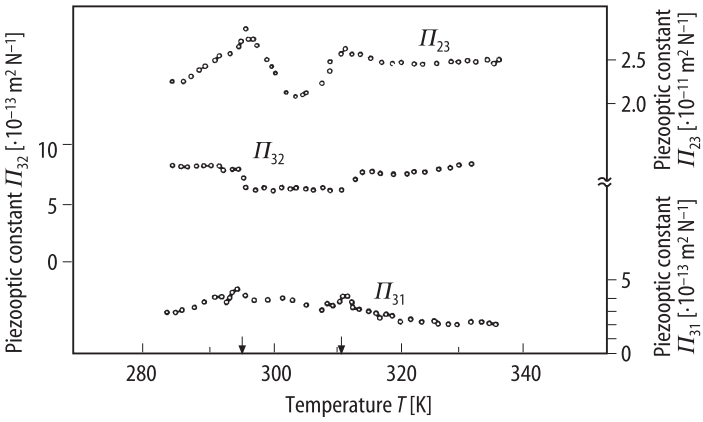

Fig. 55A-3-006. $[(CH_3)_2NH_2]_2ZnCl_4$. Π_{23}, Π_{31}, Π_{32} vs. T [90Vlo]. $\Pi_{\lambda\mu}$: piezooptic constant for T. $\lambda = 6328$ Å.

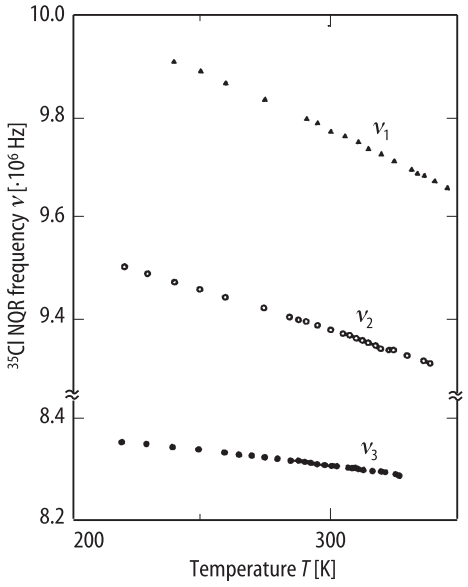

Fig. 55A-3-007. $[(CH_3)_2NH_2]_2ZnCl_4$. ν vs. T [90Yam]. ν: ^{35}Cl NQR frequency. Below RT, observation was made only with decreasing temperature.

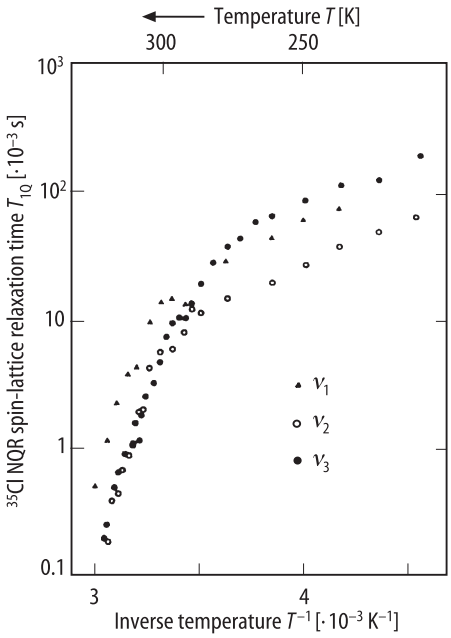

Fig. 55A-3-008. $[(CH_3)_2NH_2]_2ZnCl_4$. T_{1Q} vs. T^{-1} [90Yam]. T_{1Q}: ^{35}Cl NQR spin-lattice relaxation time for NQR lines ν_1, ν_2 and ν_3 in Fig. 55A-3-007.

References

86Bob Bobrova, Z.A., Varikash, V.M.: Dokl. Akad. Nauk BSSR **30** (1986) 510.

87Vas Vasil'ev, V.E., Rudyak, V.M., Bobrova, Z.A., Varikash, V.M.: Fiz. Tverd. Tela **29** (1987) 1539; Sov. Phys. Solid State (English Transl.) **29** (1987) 882.

89Ole Oleshchuk, A.Yu., Kiosse, G.A., Bobrova, Z.A., Shuvalov, L.A., Malinovskii, T.I.: Kristallografiya **34** (1989) 1146; Sov. Phys. Crystallogr. (English Transl.) **34** (1989) 690.

90Vlo Vlokh, O.G., Kapustyanyk, V.B., Polovinko, I.I., Sveleba, S.A., Varikash, V.M., Bobrova, Z.A.: Zh. Prikl. Spektrosk. **52** (1990) 785; J. Appl. Spectrosc. (English Transl.) **52** (1990) 527.

90Yam Yamamoto, H., Ishikawa, A., Asaji, T., Nakamura, D.: Z. Naturforsch. **45a** (1990) 464.

91Tor Torgashev, V.I., Yuzyuk, Yu.I., Rabkin, L.M., Durnev, Yu.I., Bobrova, Z.A.: Phys. Status Solidi (b) **168** (1991) 317.